Mecánica Computacional Vol. XXI, pp. 2593–2605
S. R. Idelsohn, V. E. Sonzogni and A. Cardona (Eds.)
Santa Fe–Paraná, Argentina, October 2002

COMPUTATIONAL MODEL FOR NON-ISOTHERMAL MELT SPINNING FLOWS: THE LOW TAKE UP VELOCITY RANGE

Mariel L. Ottone, Marta B. Peirotti and Julio A. Deiber

Instituto de Desarrollo Tecnológico para la Industria Química
(INTEC-UNL-CONICET)
Güemes 3450, 3000 Santa Fe, Argentina
e-mail: treoflu@ceride.gov.ar

Key words: Non-isothermal spinning flows, finite differences, stress and thermal fields, rheometric extensional viscosity, process extensional viscosity.

Abstract. *This work shows the interrelation between non-isothermal melt spinning flows and the isothermal extensional flow described through rheometry. This analysis uses the iterative numerical algorithm presented by Ottone and Deiber[1] for non-isothermal melt spinning flows in the low take up velocity range. The results obtained for two take up velocities (1500 and 2500 m/min) are then shown in the extensional rheometric map composed by the lines of the steady state rheometric extensional viscosity as function of the extensional rate at different parametric temperatures. Then the search of scaling functions that allows one the formulation of master curves relating both flows is analyzed and discussed.*

1 INTRODUCTION

Non-isothermal melt spinning flows at low take up velocities can be modeled by considering a filament of polymer melt continuously drawn and simultaneously cooled with air in order to obtain a solidified yarn. In this sense all the filaments found in the spinneret are assumed to achieve the same properties during the spinning process. These filaments compose the synthetic fiber in the bobbin (Figure 1 shows a scheme for this operation involving one filament only). Melt spinning is a basic non-isothermal process in the production of synthetic fibers (see, for example, Denn[2,3] and Schowalter[4]) and hence a model describing the velocity, stress and temperature fields in a filament can be useful to control the quality of the final product.

Recently, Ottone and Deiber[1] provided a computational algorithm based on finite differences to obtain the axial velocity profile and the thermal and stress fields in the 2-D domain of the filament. In this work, the perturbation analysis of the full spinning model reported by Henson et al.[5] was considered. This model was formulated for the low speed range (flow induced crystallization was not considered) through a regular perturbation analysis that included the slenderness approximation associated to long fibers of very small diameters. Therefore, apart from describing the relevant fields in the filament, it was also predicted phenomena present in melt fiber-spinning process like the skin-core structure.

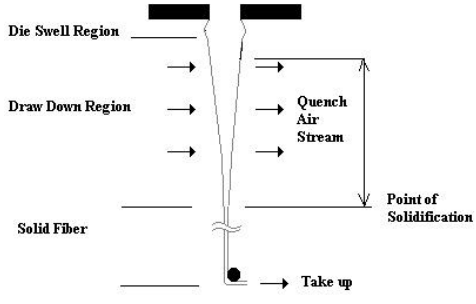

Figure 1: Scheme of the melt spinning process involving one filament.

From the above analysis, it is clear that the radial and axial stress and temperature fields in melt fiber spinning may be estimated within a consistent theoretical framework of a perturbed 2-D model that uses the slenderness approximation for the low speed range. For this purpose, a robust numerical algorithm computing the resulting momentum and energy balances coupled to constitutive equations is also available. In addition, this implies that the hybrid 1-D fluid mechanics/2-D thermal models, as they are designated by Doufas and McHugh[6], can be avoided. In the hybrid models, approximations associated to the average of non-linear terms involving temperature and stresses are required.

The purposes of the present work is to show that within the structure of the perturbed 2-D model discussed above, one can look for the interrelation between the non-isothermal spinning flow and the isothermal extensional flow described rigorously through rheometry. For this task the iterative numerical algorithm proposed by Ottone and Deiber[1] is used. The results obtained for two take up velocities (1500 and 2500 m/min) are then shown in the extensional rheometric map composed by lines of the steady state rheometric extensional viscosity versus the extensional rate at different parametric temperatures. Then the search of scaling functions that allows one the formulation of master curves relating both flows is analyzed and discussed.

The discrete non-isothermal melt spinning model is expressed in finite differences, which involve the implicit tri-diagonal algorithm for the temperature field and the explicit-implicit backward differences for the stresses. Fine meshes can be generated to the required precision (for instance, 100 radial nodes and axial step sizes of 10^{-5} m).

The relation between isothermal extensional flow and other flow kinematics, like shear flows, has been of interest since the early stages of rheometry with the purpose of evaluating the extensional viscosity (rheometric function) through other simple kinematics attained easily in experimental programs. At present, it is known that within the isothermal point of view this target is difficult to achieve[7]. It is also clear that experimental data of the steady state extensional viscosity of polymer melts at different temperatures are rather difficult to obtain. Therefore, in this context of analysis, our results provide a new insight to this basic problem when non-isothermal melt spinning flows are considered. The analysis can be done only by using a constitutive model as a reference framework because the amount of experimental data required for this purpose is not available. Thus, we use here the Phan-Thien and Tanner viscoelastic constitutive equation, which is appropriate to describe extensional flows. The study is carried out for polyethylene therephtalate (PET) which is a typical polymer used in the commercial production of fibers.

2 BASIC EQUATIONS

In this section we present briefly the non-isothermal melt spinning model formulated for the steady state regime, (a full description is already published[1]). Since the polymer is considered incompressible, the mass balance implies,

$$\left(\underline{\nabla} \cdot \underline{v}\right) = 0 \tag{1}$$

where $\underline{v}$ is the velocity vector. The balance of momentum in the filament is expressed,

$$\rho \underline{v} \cdot \underline{\nabla v} = -\underline{\nabla} p + \underline{\nabla} \cdot \underline{\underline{\tau}} + \rho \underline{g} \tag{2}$$

where ρ is the polymer density, p is the pressure field, $\underline{g}$ is the gravity vector and $\underline{\underline{\tau}}$ is the extra stress tensor considered symmetric throughout this work. The energy balance in the filament is,

$$\rho c_v \underline{v} \cdot \underline{\nabla} T = -\underline{\nabla} \cdot \underline{q} + \underline{\underline{D}} : \underline{\underline{\tau}} \tag{3}$$

where $c_v = a + bT$ is the polymer thermal capacity and T is the temperature field (temperature T is expressed in °C throughout this work). In Eq. (3), $\underline{q} = -k_s \cdot \underline{\nabla} T$ is the heat flux vector, k_s is the thermal conductivity and $\underline{\underline{D}} : \underline{\underline{\tau}}$ is the mechanical power. This term involves the rate of deformation tensor $\underline{\underline{D}} = \left(\underline{\nabla} v + \underline{\nabla} v^T\right)/2$ which is a function of the fluid kinematics $\underline{v}(r,z) = v_z \underline{e}_z + v_r \underline{e}_r$, where v_z and v_r are the axial and radial components of the velocity vector, respectively, in the cylindrical coordinate system.

To complete the formulation of the spinning model, the viscoelastic stress $\underline{\underline{\tau}}_p$ is required, which is a part of the total extra stress tensor $\underline{\underline{\tau}} = \underline{\underline{\tau}}_p + \underline{\underline{\tau}}_s$, where $\underline{\underline{\tau}}_s = 2\eta_s \underline{\underline{D}}$ is associated to retardation effects. In this sense, one expresses,

$$\underline{\underline{\tau}}_p + \lambda \frac{\delta}{\delta t} \underline{\underline{\tau}}_p = 2\lambda G \underline{\underline{D}} \tag{4}$$

for the Phan-Thien and Tanner model (PTTM).[8] In Eq. (4),

$$\frac{\delta}{\delta t} \underline{\underline{\tau}}_p = \frac{D}{Dt} \underline{\underline{\tau}}_p - \underline{\underline{L}} \cdot \underline{\underline{\tau}}_p - \underline{\underline{\tau}}_p \cdot \underline{\underline{L}}^T - \underline{\underline{\tau}}_p \frac{D \ln T}{Dt} \tag{5}$$

is the Gordon-Schowalter[9,10] non-affine time-convective derivative, where the effect of the thermal history is added through the term $D\ln T / Dt$. Also $\underline{\underline{L}} = \underline{\nabla} \cdot \underline{v} - \chi \underline{\underline{D}}$ is the effective velocity gradient tensor. We define $\eta_s = \eta_p (1-\alpha)/\alpha$ and $\eta_p = \lambda G$, hence the instantaneous elastic response of the model can be obtained for $\alpha = 1$.[11]

Since the rheological model gets the linear viscoelastic response at the asymptotic limit of small shear rates, the relaxation time can be expressed $\lambda = \lambda_o(T) / K\left(T, tr\underline{\underline{\tau}}\right)$ where $\lambda_o = \lambda_{oo}\, exp\left[-11.9755 + 6802/(T+273)\right]$ as reported by Gregory and Watson.[12] Here, the PTTM considers a relaxation time that is a function of the stress tensor through the function $K = exp\left[\xi tr\underline{\underline{\tau}}/G\right]$. In this context of analysis the relaxation modulus is also allowed to change with temperature according to $G = G_o\,(T/T_r)$ where T_r is the reference temperature.

Rheometric characterizations of this rheological model were carried out by following the same procedure described by Ottone and Deiber[13] to evaluate the rheological parameters of the PET melt with experimental data reported by Gregory and Watson[12] involving the shear rate flow of a sample that had the same intrinsic viscosity as the PET used by George.[14] The thermo-physical properties required above are also reported in our work.[13]

The appropriate set of boundary conditions to solve Eqs (1) to (5) are taken directly from Denn[2] and the numerical method used is that proposed by Ottone and Deiber.[1]

3 RHEOMETRIC AND PROCESS ELONGACIONAL VISCOSITIES

To analyze the relation between non-isothermal melt spinning flows[15,16] and the isothermal extensional flow (the target of this work), we have to define the rheometric and process extensional viscosities. While the first viscosity is a rheometric function under isothermal conditions, the second one is obtained from the non-isothermal melt spinning process where a radial averaged and axial varying temperature profile is obtained. Therefore, throughout the rest of this work, the use of a super-index p to indicate any variable evaluated with the melt spinning model is appropriate. It is also clear that the process variables, $\eta_e{}^p$, $\dot{\varepsilon}^p$ and T^p cannot be placed in the rheometric extensional map (the extensional viscosity η_e versus the extensional rate $\dot{\varepsilon}$ for different parametric temperatures T) without further considerations. For this task to be possible, the "equivalent rheometric variable", designated here with a super index (*), should be defined. These properties allow one to plot the results of the melt spinning process (trajectories) in the extensional rheometric map defined with the true rheometric variables η_e, $\dot{\varepsilon}$ and T.[17]

In this section we use a cylindrical coordinate system (z,r,θ) placing the z-axis along the filament from the maximum swelling to the take up roll (Figure 1). Also, it is should be observed that the numerical method used[1] involves a coordinate transformation defining new variables (Z,ζ,θ) with $Z = z$. Therefore, the extensional viscosity is expressed[7],

$$\eta_e(T,\dot{\varepsilon}) = \frac{\left(\tau^{zz} - \tau^{rr}\right)}{\dot{\varepsilon}} \tag{6}$$

where $\dot{\varepsilon} = \dfrac{\partial v_z}{\partial Z}$ is constant when steady rheometric conditions are achieved. In a similar way, one can also define the process extensional viscosity,

$$\eta_e{}^p\left(T^*,\dot{\varepsilon}^p\right) = \frac{\left(\tau^{zz} - \tau^{rr}\right)^p}{\dot{\varepsilon}^p} \tag{7}$$

where the process extensional rate is obtained from $\dot{\varepsilon}^p = \left(\dfrac{\partial v_z}{\partial Z}\right)^p$. In Eq. (7), T^* is the equivalent rheometric temperature, which results from the extensional rheometric map with the values of $\eta_e{}^p$ y $\dot{\varepsilon}^p$. It is understood that that temperature T^* is different from the process temperature T^p that corresponds to values $\eta_e{}^p$ and $\dot{\varepsilon}^p$. Thus, the equivalent rhemetric variables take the value from the extensional rheometric map and correlates with the other two remaining process variables at the same axial position.

It is also clear that we can obtain three different equivalent rheometric variables for the melt spinning process: T^*, η_e^* y $\dot{\varepsilon}^*$. Consequently, the equivalent rheometric extensional viscosity is,

$$\eta_e^*\left(T^p,\dot{\varepsilon}^p\right)=\frac{\left(\tau^{zz}-\tau^{rr}\right)^*}{\dot{\varepsilon}^p} \tag{8}$$

and is obtained with T^p and $\dot{\varepsilon}^p$. Finally, the equivalent rheometric extensional rate comes from the extensional rheometric map with the values T^p and $\eta_e{}^p$ as follows:

$$\dot{\varepsilon}^*\left(T^p,\eta^p\right)=\left(\frac{\partial v_z}{\partial Z}\right)^* \tag{9}$$

where the process extensional viscosity is,

$$\eta_e{}^p\left(T^p,\dot{\varepsilon}^p\right)=\frac{\left(\tau^{zz}-\tau^{rr}\right)^p}{\dot{\varepsilon}^p} \tag{10}$$

One should observe that Eqs (7) and (10) refers to the same value of extensional viscosity but they have associated different temperatures.

Once the interplay between process and extensional rheometric variables has been defined, the search of master curves are carried out by using the thermal shift factor a_T, which is expressed,

$$a_T=\frac{\lambda_o(T)}{\lambda_o(T_r)}=\frac{\lambda_o(T)}{\lambda_{oo}}=exp\left[-11.9755+\frac{6802.1}{(T+273)}\right] \tag{11}$$

for the PET. Thus, Eq. (11) can be used to find either the rheometric shift factor a_T and process shift factor $a_T{}^p$ when data of T and T^p are available, respectively.

4 RESULTS AND DISCUSSION

Figures 2 and 3 show numerical predictions with the PTTM of the axial velocity v_z and the radial averaged temperature $\langle T\rangle$ for two different take up velocities (1500 and 2500 m/min) to illustrate the data available in the search of the master curves proposed in this work.

In previous works[1,13] we also showed that good agreement between numerical results and experimental data is obtained for take up velocities of 3000, 2000 and 1000 m/min.

Figure 4 shows trajectories of the melt spinning process in the extensional rheometric map for the two take up velocities of Figures 2 and 3, when the equivalent rheometric extensional rate is used (Eq. (9)). An interesting result can be obtained when the curves of Figure 4 are presented through a master curve by using Eq. (11) to reduce the extensional rate at the reference temperature. Thus, Figure 5 shows that the rheometric and process master curves become superposed and that the melt spinning process should be within the range where the rheometric extensional viscosity is increasing with extensional rate. The reference temperature for these calculations is 295 ^{o}C.

Nevertheless, this is not necesarily the only master curve that can be achieved because we have also defined other equivalent rheometric variables. For instance, Figure 6 shows trajectories of the melt spinning process in the extensional rheometric map for the two take up velocities of Figures 2 and 3, when the equivalent rheometric extensional viscosity is used (Eq. (8)) and hence, Figure 7 shows that the rheometric and process master curves become superposed again, but in this case the melt spinning process is within the range where the rheometric extensional viscosity is decreasing. From the two types of master curves discussed above one should observe that the equivalent rheometric extensional viscosity is rather difficult to interpret and further studies are required in this sense.

To complete the anlaysis involving the equations of the previous section, Figure 8 shows trajectories of the melt spinning process in the extensional rheometric map for the two take up velocities of Figures 2 and 3, when the equivalent rheometric temperature is used (Eq. (7)) and hence, Figure 9 shows that the rheometric and process master curves become superposed again, but in this case the melt spinning process is within the same range as for the case in which the equivalent rheometric extensional rate is used. This certainly indicates that both reduction process to a master curve are similar.

Finally, Figure 10 shows that the rheometric and process master curves do not coincide when the concept of equivalent rheometric temperature is not taken into account (Eq. (7)). Although these master curves are obtained using Eq. (11) to reduce the extensional rate at the reference temperature, one observes that the effect of different thermal histories become evident. Thus, the rheometric extensional viscosity is higher than those of the process at different take up velocities for the reported reference temperature. However, for low values of extensional rate the three curves tend asymptotically to the Trouton value.

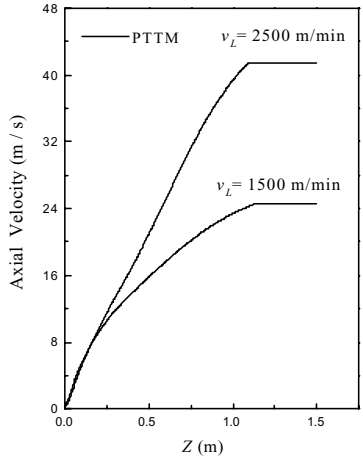

Figure 2: Numerical predictions with the PTTM of the axial spinning velocity v_z at two different take up velocities for the PET melt.

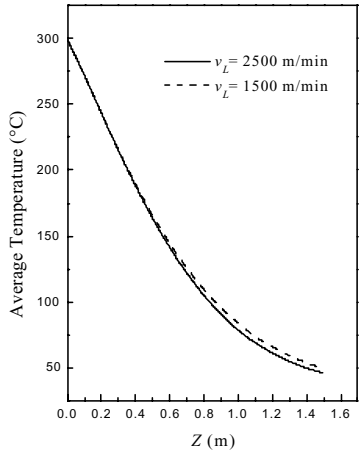

Figure 3: Numerical predictions with the PTTM of the average temperature $\langle T \rangle$ at two different take up velocities for the PET melt.

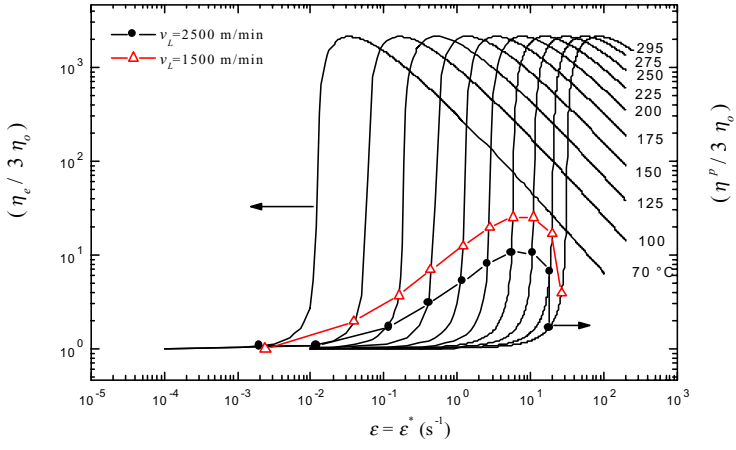

Figure 4: Trajectories of the melt spinning process (lines with symbols) in the extensional rheometric map (full lines) for two take up velocities when the equivalent rheometric extensional rate is defined.

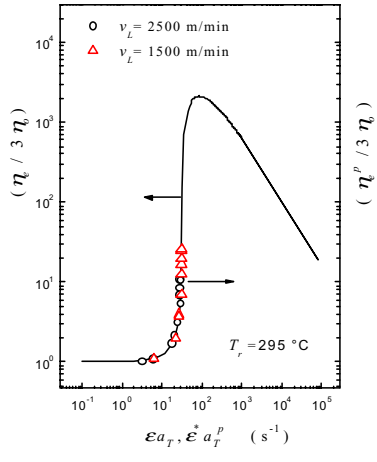

Figure 5: Rheometric master curve (full line). Symbols belong to the reduced trajectories of the melt spinning process in the extensional rheometric map (full lines) for two take up velocities when the equivalent rheometric extensional rate is defined.

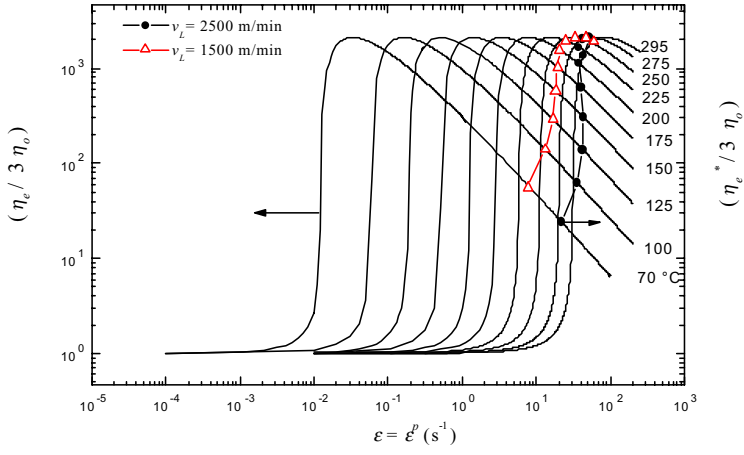

Figure 6: Trajectories of the spinning process (lines with symbols) in the extensional rheometric map (full lines) for two take up velocities when the equivalent rheometric extensional viscosity is defined.

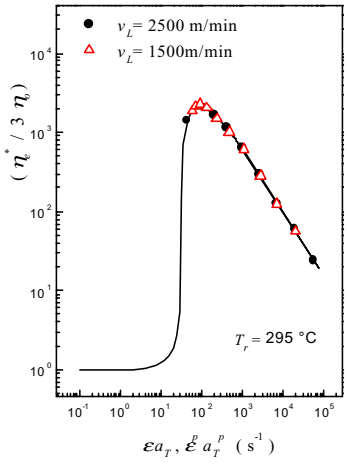

Figure 7: Rheometric master curve (full line). Symbols belong to the reduced trajectories of the melt spinning process in the extensional rheometric map for two take up velocities when the equivalent rheometric extensional viscosity is defined

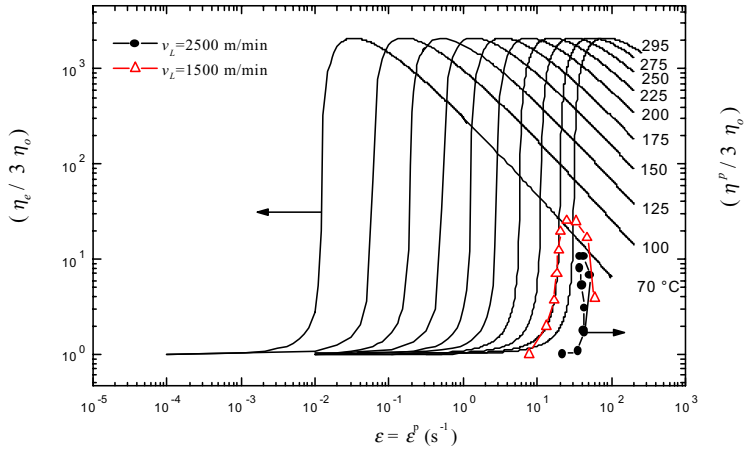

Figure 8: Trajectories of the spinning process (lines with symbols) in the extensional rheometric map (full lines) for two take up velocities when the equivalent rheometric temperature is defined.

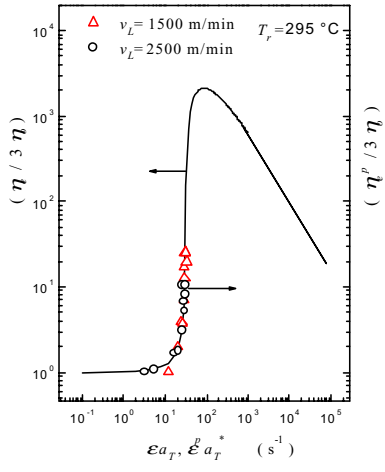

Figure 9: Rheometric master curve (full line). Symbols belong to the reduced trajectories of the melt spinning process in the extensional rheometric map for two take up velocities when the equivalent rheometric temperature is defined

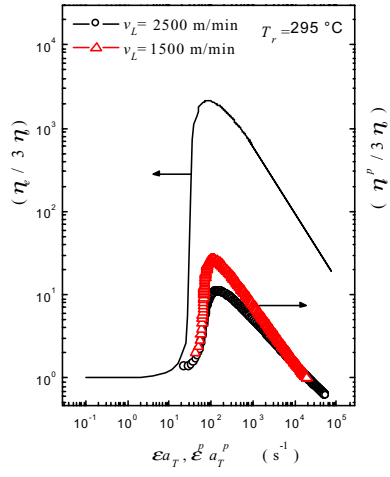

Figure 10: Rheometric master curve (full line). Symbols belong to the reduced trajectories of the melt spinning process in the extensional rheometric map (full lines) for two take up velocities when the equivalent rheometric temperature is defined.

5 CONCLUSIONS

Numerical results concerning velocity, temperature and stresses of non-isothermal melt spinning flows can be placed as process trajectories in the rheometric extensional map composed by the extensional viscosity η_e as function of the extensional rate $\dot{\varepsilon}$ for different parametric temperatures *T*. The interplay between these flows is possible when the equivalent rheometric variables are defined in terms of the corresponding pair of process variables at each axial position. The three cases considered yield coincident rheometric and process master curves when the extensional rate is reduced with the appropriate thermal shift factor.

6 ACKNOWLEDGMENTS

The authors are thankful for financial aid received from the CONICET (Consejo Nacional de Investigaciones Científicas y Técnicas, Argentina) PIP 4811/97 and the Secretaría de Ciencia y Técnica de la UNL (Universidad Nacional del Litoral, Argentina) Programación CAI+D 96.

7 REFERENCES

[1] M.L. Ottone and J.A. Deiber, "A numerical method for the viscoelastic melt spinning model with radial resolutions of temperature and stress field", *Industrial & Engineering Chemistry Research*, in press (2002).
[2] M.M. Denn, "Continuous drawing of liquids to form fibers", *Ann. Rev. Fluid Mech*., **12**, 365-387 (1980).
[3] M.M. Denn, *Computational analysis of polymer processing*; Pearson, J. R. A., Richardson, S. M. Eds.; Applied Science Publishers: New York, (1983).
[4] W.R. Schowalter, *Mechanics of non-newtonian fluid,* Pergamon Press: New York, (1978).
[5] G.M. Henson, D. Cao, S.E. Bechtel and M.G. Forest, "Thin-filament melt spinning model with radial resolution of temperature and stress", *J. Rheol*., **42**, 329- 360 (1998).
[6] A.K. Doufas and A.J. McHugh, "Two-dimensional simulation of melt spinning with a microstructural model for flow-induced crystallization", *J. Rheol*., **45**, 403-420 (2001).
[7] K. Walters, *Rheometry*, J. Wiley & Sons: New York, (1975).
[8] R.G. Larson, *Constitutive equations for polymer melts and solutions,* Butterworths Series in Chemical Engineering; Butterworth Publishers, (1988).
[9] F. Sugeng, N. Phan-Thien and R.I. Tanner, "A study of non-isothermal non-newtonian extrudate swell by a mixed boundary element and finite element method", *J. Rheol.*, **31**, 37-58 (1987).
[10] R.J. Gordon and W.R. Schowalter, "Anisotropic fluid theory: a different approached to the dumbbell theory of dilute polymer solutions", *Trans. Soc. Rheol.*, **16**, 79-97 (1972).
[11] M.M. Denn, "Issues in Viscoelastic Flow",. *Ann. Rev. Fluid Mech.*, **22**, 13-34 (1990).
[12] D.R. Gregory and M.T. Watson, "Steady state properties of poly(ethylene terephthalate) melts", *J. Polym. Sci*., **30**, 399-406 (1970).
[13] M.L. Ottone and J.A. Deiber, "Modeling the melt spinning of polyethylene terephthalate", *J. Elast. Plast*., **32,** 119-139 (2000).
[14] H.H. George, "Model of steady-state melt spinning at intermediate take-up speeds", *Polym. Eng. Sci*., **22**, 292-299 (1982).
[15] R.K. Gupta and A.B. Metzner, "Modeling of non-isothermal polymer processes", *J. Rheol*., **26**, 181-198 (1982).
[16] M.M. Denn, "Correlations for transport coefficients in textile fiber spinning", *Ind. Eng. Chem. Res*., **35**, 2842-2843 (1996).
[17] M.L. Ottone, "Reología y transferencia de energía en el proceso de hilado del poliester tereftálico", tesis doctoral, Universidad Nacional del Litoral, Santa Fe, Argentina (2001).